University of Glasgow

DEPARTMENT OF

AEROSPACE ENGINEERING

Identification of Autogyro Longitudinal Stability and Control Characteristics From Flight Test

S. S. Houston

Identification of Autogyro Longitudinal Stability and Control Characteristics From Flight Test

S. S. Houston

Identification of Autogyro Longitudinal Stability and Control Characteristics From Flight Test

S. S. Houston[1]

Abstract

This Paper presents an analysis of test data recorded during flight trials of an autogyro. This class of rotary-wing aircraft has found limited application in areas other than sport or recreational flying. However, the accident rate is such that a study of the configuration's stability and control characteristics is timely, and in addition substantive data is required for a new airworthiness and design standard that is under development. The Paper presents a unique coupling of established parameter estimation techniques with data from a class of aircraft that has received no attention in the contemporary literature. As a consequence, the Paper helps to consolidate the status of system identification as a powerful tool in the analysis of rotorcraft engineering problems. It is concluded that robust estimates of the longitudinal stability and control derivatives have been identified, indicating benign and "classical" longitudinal stability and control characteristics. However, unlike most helicopters, the rotorspeed degree of freedom must be included in the model structure.

[1]Member AIAA
Lecturer, Dept. of Aerospace Engineering
The University of Glasgow
Glasgow
Scotland
G12 8QQ

Nomenclature

A, B	state-space system and control matrices
u, w	velocity components along longitudinal, vertical body axes, m/s^2
u_{probe}, w_{probe}	velocity components along longitudinal, vertical air data probe axes, m/s^2
p, q, r	angular velocity components about body axes, rad/s
$x_{vane}, y_{vane}, z_{vane}$	angle of attack and sideslip vane location in body axes, m
x_{cg}, y_{cg}, z_{cg}	aircraft centre-of-mass position in body axes, m
$\underline{x}, \underline{u}$	state and control vectors
$\underline{x}(\omega), \underline{u}(\omega)$	Fourier-transformed state and control vectors
Re[], Im[]	real and imaginary components of []
i	imaginary operator
X_u, X_w, etc	longitudinal body axis acceleration derivatives, 1/s
Z_u, Z_w, etc	vertical body axis acceleration derivatives, 1/s
M_u, M_w, etc	pitching moment derivatives, 1/(ms)
T_u, T_w, etc	rotor torque derivatives, rev/min/(m)
T, T_p	rotor, propeller thrust, N
$T(u,w)$	rotor thrust in (u,w) disturbed flight, N
$\alpha_{vane}, \beta_{vane}$	angle of attack and sideslip measured at vane location, rad
Δf	frequency increment, rad/s
Δt	time increment, s
η_s	longitudinal stick position, % (0% fully forward)
Ω	rotorspeed, rev/min
ω	frequency, rad/s

Introduction

There are a wide range of configurations in the class of aircraft known as rotorcraft. The helicopter is the most common type, finding widespread application in commercial and military aviation. The autogyro (or gyroplane), however, is an increasingly popular machine in sport and recreational flying, having found no practical application in contemporary commercial or military roles.

Currently, most if not all types of autogyro are in the homebuilt, or experimental category. The study of the configuration's flight mechanics is timely, given the accident rate suffered by the aircraft, e.g. Ref. 1. This, together with the increase in light autogyro flying in the U.K., has heightened interest in this class of aircraft, and a new airworthiness and design standard (BCAR Section T) has been published by the U.K. Civil Aviation Authority, Ref. 2.

However, there is little substantive data at present to support the design standard, and the literature has not, until recently, addressed stability and control (Ref. 3). The objective of this Paper is therefore to contribute to a sparse literature on the subject of autogyro flight mechanics, thereby directly supporting BCAR Section T. The specific aims of the work are: to explore the application, to the autogyro, of previous research in rotorcraft system identification; to obtain robust estimates of longitudinal stability and control derivatives; and to use these derivatives to assess the nature of the flight dynamics of autogyros.

Background

The autogyro helped to pave the way for the development of the helicopter, introducing cyclic pitch control and blades attached to the rotor hub by means of a hinge. Unfortunately, with the one exception of Ref.3, the literature has not hitherto addressed stability and control. The literature on autogyros nonetheless is considerable, Refs. 4-14 for example. However, in a contemporary context, this work is now primarily of historical significance. It provides the basis of the understanding of autogyro flight, but does not address the issues of stability and control. Examination of the literature shows a logical development of the study of autogyros, from the elementary theory of autogyro flight, to an analysis of aerodynamics and performance and ultimately rotor behaviour, but only for steady flight. Interest then apparently waned and the next logical stage in the study of the autogyro i.e. stability and control, was not examined. For example, the work of Glauert includes the derivation of simple expressions for rotorspeed as a function of loading and axial velocity, Ref. 4. Wheatley, Ref. 10 derived expressions for the flapping angles required for equilibrium flight, presenting results that show how coning, longitudinal and lateral flap angles vary with flight condition. Nowadays, these analyses would be recognisable as classical rotary-wing theory and analogous to that found in helicopter text books. Wheatley even examined higher harmonic components of blade flapping behaviour, Ref. 12.

It is in this context that autogyro flight trials and the associated data analysis methods, were planned. There is an extensive literature on system identification and parameter estimation, and application to the rotorcraft problem is well documented, e.g. Refs. 15-20. Tischler in particular has argued strongly in favour of the merits of frequency-domain identification, specifically directed towards the synthesis of non-parametric frequency responses. The repeatability and consistency achieved indicates that the frequency domain approach is robust.

The approach taken in this Paper is to adopt a frequency-domain equation-error method using linear regression, to synthesise conventional 3 degree-of-freedom stability and control derivatives. This model structure is familiar to flight dynamicists, thereby facilitating general insight into fundamental behaviour of the autogyro. Specific derivatives are directly related to individual, or group, effects that would otherwise be hidden in the aggregate presentation of a frequency response. The equation error method has limitations, as described in Refs. 15 and 18, although working in the frequency domain minimises some of the difficulties. The advantage is the simplicity of the approach, in concept and application. It is argued that sound engineering judgement, together with good experiment and installation design and execution, can produce good results with a frequency-domain equation-error approach.

Aircraft and Experimental Installation

The aircraft used in this study was the VPM M16 autogyro, Figure 1. It is of Italian origin, produced in kit form for assembly by the owner. The maximum all-up mass is 450 kg. The aircraft is powered by a four-cylinder two-stroke engine driving a three-bladed fixed pitch propeller. For helicopter engineers not familiar with autogyros, the rotor system is of an interesting configuration, typical of this class of aircraft. The two main rotor blades are bolted to a teeter bar, suspended from a teeter bolt. The blades are untwisted, and no cyclic pitch can be applied. This hub assembly is mounted on a spindle, about 200mm long, and this spindle pivots about its lower end to tilt the entire rotor fore and aft and laterally to effect pitch and roll control, respectively. In this regard, the aircraft could be classed as a tilt-rotor.

The experimental installation consisted of a digital on-board recording system, operating at 10 Hz. A nose-mounted air data probe containing sideslip and angle of attack vanes was fitted, and an inertial unit measured angular velocities about three axes, and linear accelerations along these axes. A separate unit was used to measure roll and pitch angles . Pilot control positions were measured using potentiometers. Rotorspeed was also recorded. The front seat and flight controls were removed to accommodate the system.

The autogyro presents a particular challenge, in addition to those normally met with helicopter system identification. The aircraft is light, which demands stringent limits on atmospheric conditions during the tests. Solo operation of this aircraft was essential due to the mass and space restrictions imposed by the instrumentation system, placing particular demands on the test pilot's flying skill in relation to the quality of test inputs.

Data Analysis and Model Synthesis

The model structure for which coefficients are to be identified, is of conventional state-space form, i.e.

$$\dot{\underline{x}} = A\underline{x} + B\underline{u}$$

where

$$A = \begin{bmatrix} X_u & X_w & X_q & X_\theta & X_\Omega \\ Z_u & Z_w & Z_q & Z_\theta & Z_\Omega \\ M_u & M_w & M_q & M_\theta & M_\Omega \\ 0 & 0 & 1 & 0 & 0 \\ \mathrm{T}_u & \mathrm{T}_w & \mathrm{T}_q & \mathrm{T}_\theta & \mathrm{T}_\Omega \end{bmatrix} \quad , \quad B = \begin{bmatrix} X_{\eta_s} \\ Z_{\eta_s} \\ M_{\eta_s} \\ 0 \\ \mathrm{T}_{\eta_s} \end{bmatrix}$$

This constitutes the longitudinal subset of the conventional 3 DOF rigid-body flight mechanics model, with the important (and unique) addition of the rotorspeed degree of freedom. The rigid body states are taken to be with respect to the usual mutually orthogonal, right-handed frame of reference whose origin is at the centre of mass.

The angular quantities in the state vector, and the control position, are all measured directly. The translational velocities u and w are obtained from airspeed, sideslip and angle of attack data measured at the nose-mounted boom, as follows.

$$u = u_{probe} - q(z_{vane} - z_{cg}) + r(y_{vane} - y_{cg})$$
$$w = w_{probe} - p(y_{vane} - y_{cg}) + q(x_{vane} - x_{cg})$$

and

$$u_{probe} = \frac{V_f \cos\beta_{vane}}{\sqrt{1 + \tan^2 \alpha_{vane}}} \quad ; \quad w_{probe} = u_{probe} \tan \alpha_{probe}$$

The time histories of each variable were then converted into frequency domain information using a Discrete Fourier Transform, Ref. 20, given by

$$X(k\Delta f) = \Delta t \sum_{n=0}^{N-1} x_n e^{-i2\pi(kn)/N}; \quad k = 0,1,2,\ldots,N-1$$

which gives real and imaginary parts of X ,

$$\mathrm{Re}[X(k\Delta f)] = \Delta t \cos(2\pi(kn)/N); \quad \mathrm{Im}[X(k\Delta f)] = -\Delta t \sin(2\pi(kn)/N)$$

The quality of these frequency domain data can be enhanced by standard processing techniques such as applying overlapped and tapered windows to the data, as recommended by Tischler, Ref. 20.

Each degree of freedom can then be treated separately, and formulation as a linear regression problem allows estimation of the coefficients. The state-space description is converted to the frequency domain, i.e.

$$i\omega\, \underline{x}(\omega) = A\underline{x}(\omega) + B\underline{u}(\omega)$$

Note that this assumes that any process noise is zero. The real parts on each side can be equated, as can the imaginary parts, to give two matrix equations that the A and B coefficients must satisfy, viz.

$$-\omega\,\mathrm{Im}[\underline{x}(\omega)] = A(\mathrm{Re}[\underline{x}(\omega)]) + B(\mathrm{Re}[\underline{u}(\omega)])$$
$$\omega\,\mathrm{Re}[\underline{x}(\omega)] = A(\mathrm{Im}[\underline{x}(\omega)]) + B(\mathrm{Im}[\underline{u}(\omega)])$$

The pitching moment equation for example, is then expressed as two equations

$$-\omega\,\mathrm{Im}[q(\omega)] = M_u\,\mathrm{Re}[u(\omega)] + M_w\,\mathrm{Re}[w(\omega)] + M_q\,\mathrm{Re}[q(\omega)] + M_\theta\,\mathrm{Re}[\theta(\omega)] + M_\Omega\,\mathrm{Re}[\Omega(\omega)] + M_{\eta_s}\,\mathrm{Re}[\eta_s(\omega)]$$

$$\omega\,\mathrm{Re}[q(\omega)] = M_u\,\mathrm{Im}[u(\omega)] + M_w\,\mathrm{Im}[w(\omega)] + M_q\,\mathrm{Im}[q(\omega)] + M_\theta\,\mathrm{Im}[\theta(\omega)] + M_\Omega\,\mathrm{Im}[\Omega(\omega)] + M_{\eta_s}\,\mathrm{Im}[\eta_s(\omega)]$$

The other degrees of freedom are in a similar form.

Results

Two types of input were performed at speeds of between 30 and 70 mph, from a level flight equilibrium condition: a doublet-type input was used to excite the short-period response, and the standard technique of displacing the stick to provoke a speed change before returning it to trim was used to excite any phugoid. Figure 2 shows typical time histories, recorded from a test performed specifically to excite the phugoid mode. In addition, frequency sweep tests were conducted at 70 mph. This type of input proved difficult to perform at 30 and 50 mph due to the ineffectiveness of the trim system on the aircraft at all but the upper end of the level flight speed range. Figure 3 illustrates a typical frequency sweep.

An important aspect in any system identification study is the *identifiability* of the estimated parameters, Refs.21, 22. This is particularly germane to the equation error approach. *Robust* estimates of the derivatives are those whose values can be judged to be invariant with the input type, estimation method or frequency range used, and for which a low standard error is calculated. *Verification* will then confirm the appropriateness of the identified model. This is usually achieved by confirming that the model will predict the response to a dissimilar control input to that used in the identification. The issue of identifiability is particularly germane to the autogyro problem as there is no literature on the vehicle's characteristics. These issues are explored next.

Derivative estimates from dissimilar input types

Data from doublet and phugoid tests were zero-meaned and concatenated to provide a 90 second record length. The longitudinal derivatives estimated using these data are compared in Tables 1-4, with derivatives estimated from a frequency sweep. The standard error associated with each derivative is given in parentheses.

Table 1 X-force derivative comparison - dissimilar input types

parameter	concatenated doublet/phugoid	frequency sweep
R	0.773	0.822
X_u	-0.012 (0.059)	0.047 (0.025)
X_w	-0.328 (0.159)	-0.268 (0.058)
X_q	3.704 (2.721)	-1.169 (1.380)
X_θ	-20.327 (3.919)	-10.632 (0.851)
X_Ω	-0.021 (0.013)	-0.025 (0.006)
X_{η_s}	-0.037 (0.030)	-0.001 (0.013)

Consistent estimates of the derivatives are obtained, particularly in the pitching moment and rotor torque equations. The correlation coefficients are also in general good. The standard error associated with each estimate is relatively small, although for frequency sweep-derived parameters the errors are significantly smaller than with the concatenated doublet/phugoid.

Table 2 Z-force derivative comparison - dissimilar input types

parameter	concatenated doublet/phugoid	frequency sweep
R	0.891	0.706
Z_u	-0.251 (0.028)	-0.128 (0.024)
Z_w	-0.812 (0.074)	-0.565 (0.057)
Z_q	28.480 (1.270)	26.446 (1.350)
Z_θ	-3.070 (1.829)	4.060 (0.832)
Z_Ω	-0.020 (0.006)	-0.065 (0.006)
Z_{η_s}	-0.109 (0.014)	-0.098 (0.013)

Table 3 pitching moment derivative comparison - dissimilar input types

parameter	concatenated doublet/phugoid	frequency sweep
R	0.919	0.886
M_u	0.023 (0.003)	0.021 (0.001)
M_w	-0.065 (0.007)	-0.064 (0.003)
M_q	-1.213 (0.126)	-1.055 (0.076)
M_θ	-0.449 (0.181)	-0.294 (0.047)
M_Ω	-0.001 (0.0006)	-0.001 (0.0003)
M_{η_s}	0.029 (0.001)	0.028 (0.0007)

Derivatives that physically ought to have negligible aerodynamic or propulsion force and moment contributions (i.e. those dominated by kinematic or gravitational terms), are X_θ and Z_q . The former ought to have a value of approximately -9.81. It can be seen that in this respect, the concatenated doublet/phugoid run offers a much poorer estimate of X_θ than the frequency sweep. However, both input types give estimates of Z_q that are not only very similar, but also consistent with the mean flight speed of 28 m/s. This enhances confidence in the frequency sweep-derived Z-force derivatives, despite this equation providing the lowest correlation coefficient.

Estimates for the X-force derivative X_u are very small, with relatively large standard error. Indeed, the frequency sweep-derived value is positive. This parameter is the primary damping term in the phugoid mode, Ref. 23, and it would normally be expected to be substantially negative. Inspection of the airspeed time histories in Figure 2 suggests consistency with the identified values of X_u, in that there is little apparent damping of airspeed during the phugoid oscillation. This behaviour has been attributed to the propeller thrust varying with airspeed, for the fixed throttle position used.

The pitching moment derivatives M_u , M_w and M_q describe an aircraft with classical longitudinal stability characteristics. Speed stability is positive ($M_u > 0$), angle of attack stability is positive ($M_w < 0$) and the primary pitch damping is positive ($M_q < 0$). Figure 4 shows a comparison of the identified pitching moment equation's fit of the Fourier-transformed frequency sweep data. The fit is good across the frequency range

Table 4 rotor torque derivative comparison - dissimilar input types

parameter	concatenated doublet/phugoid	frequency sweep
R	0.910	0.966
T_u	1.373 (0.166)	1.378 (0.042)
T_w	5.324 (0.628)	5.901 (0.126)
T_q	12.590 (12.419)	7.679 (3.076)
T_θ	0 - fixed	0 - fixed
T_Ω	-0.129 (0.029)	-0.085 (0.007)
T_{η_s}	0.305 (0.129)	0.314 (0.030)

Derivative estimates from fits over dissimilar frequency ranges

Suitable choice of frequency range across which the identification is to be conducted, is important for two reasons. First, too small a frequency range and insufficient information may be available to fully specify the parameters in the model structure. Second, too large a frequency range, and dynamics unmodelled by the 4 DOF structure may distort the values. Derivative estimates from the frequency sweep data were obtained by regression over 0.5 and 1Hz, and these results are compared in Tables 5-8.

The pitching moment and rotor torque derivatives show little variability with the frequency range used. The force derivatives show some variation, but it is not

significant enough to produce substantially dissimilar dynamic characteristics. There is some evidence that 0.5 Hz is insufficient to fully specify the force derivatives. The

Table 5 **X-force derivative comparison - dissimilar regression frequency range**

parameter	0.5 Hz	1.0 Hz
R	0.902	0.822
X_u	0.112 (0.034)	0.047 (0.025)
X_w	-0.248 (0.065)	-0.268 (0.058)
X_q	-6.137 (2.374)	-1.169 (1.380)
X_θ	-10.467 (0.852)	-10.632 (0.851)
X_Ω	-0.025 (0.006)	-0.025 (0.006)
X_{η_s}	0.053 (0.024)	-0.001 (0.013)

Table 6 **Z-force derivative comparison - dissimilar regression frequency range**

parameter	0.5 Hz	1.0 Hz
R	0.786	0.706
Z_u	-0.092 (0.029)	-0.128 (0.024)
Z_w	-0.621 (0.055)	-0.565 (0.057)
Z_q	23.301 (2.003)	26.446 (1.350)
Z_θ	3.489 (0.719)	4.060 (0.832)
Z_Ω	-0.061 (0.005)	-0.065 (0.006)
Z_{η_s}	-0.047 (0.021)	-0.098 (0.013)

parameter Z_q is reduced to a level some 30 % below the flight speed, which it should approximate. The control derivative X_{η_s} assumes a positive value, which is physically inconsistent with the effect of this control. In both cases, the standard

error associated with the 0.5 Hz estimate is increased relative to that obtained for regression over 0.5 Hz. Concern that unmodelled rotor dynamics may be distorting the derivative estimates obtained for the 1 Hz regression is allayed by the pitching moment derivatives, which are arguably the most sensitive to these effects. Parameter estimates and standard errors are very similar in both cases.

Table 7 pitching moment derivative comparison - dissimilar regression frequency range

parameter	0.5 Hz	1.0 Hz
R	0.897	0.886
M_u	0.021 (0.001)	0.021 (0.001)
M_w	-0.043 (0.003)	-0.064 (0.003)
M_q	-1.199 (0.093)	-1.055 (0.076)
M_θ	-0.203 (0.033)	-0.294 (0.047)
M_Ω	-0.001 (0.0002)	-0.001 (0.0003)
M_{η_s}	0.023 (0.001)	0.028 (0.0007)

Table 8 rotor torque derivative comparison - dissimilar regression frequency range

parameter	0.5 Hz	1.0Hz
R	0.984	0.966
T_u	1.535 (0.063)	1.378 (0.042)
T_w	6.319 (0.133)	5.901 (0.126)
T_q	-9.061 (5.036)	7.679 (3.076)
T_θ	0 - fixed	0 - fixed
T_Ω	-0.073 (0.007)	-0.085 (0.007)
T_{η_s}	0.390 (0.052)	0.314 (0.030)

Verification

Figure 5a shows verification of a model identified from frequency sweep data. The model is driven by a doublet-type input made at the same nominal flight condition. The doublet-type input was used specifically to excite the short-period mode, where the dominant responses were observed to be in pitch rate and rotorspeed. The identified model provides a very good representation of the response, but displays a feature common to verification with other runs, in that any mismatch between identified model and measurement is associated with reduction in rotorspeed.

Figure 5b shows the model's ability to simulate measured behaviour during a phugoid test. Amplitude and phase of the u velocity and rotorspeed components of the phugoid mode are well represented by the identified model. The slight mismatch in the long-period response is the result of the model result being shifted in time by about 2 s relative to the measured response. This is perhaps not surprising for two reasons. First, the correlation coefficients shown previously indicate that the model structure may only approximate observed behaviour. Second, the input required for the phugoid test produced a very substantial reduction in airspeed, which may take the identified model out of its limit of applicability. Notwithstanding this, the model does capture the substantial reduction in airspeed and rotorspeed before the control is returned to trim.

Assessment of autogyro longitudinal flight dynamics

The foregoing provides a qualitative and quantitative basis for the judgement that the identified models provide a good representation of the longitudinal flight dynamics of the VPM M16 autogyro. They can therefore be used to assess the nature of the type's stability and controllability characteristics.

Figure 6 shows the eigenvalues of the synthesised models at 30 and 70 mph. The arrows indicate the progression from low to high speed. The two oscillatory modes are consistent with the frequency and damping of classical aircraft short-period and phugoid oscillations. The aperiodic mode is that of the rotorspeed degree of freedom. Assessment of the eigenvectors of the identified A matrices indicates that rotorspeed also features significantly in the rigid-body modes. The phugoid mode is relatively insensitive to changes in airspeed. The time to half amplitude is about 30-40 sec, its period 12-15 sec. The short-period mode is less than critically-damped throughout the speed range, with a damped natural frequency of between 0.1 and 0.25 Hz. The rotorspeed mode time to half amplitude lies between 1-4 sec.

Figure 7 presents the 95% confidence, 95% probability bounds of those identified derivatives that tend to determine fundamentally the dynamic characteristics. The relatively wide boundaries associated with X_u, and the small or even positive identified values are probably due to the fact that the propeller speed variations are not included in the model structure. The other derivative estimates all exhibit much narrower bounds. The aircraft exhibits "classical" static stability characteristics ($M_u > 0$, $M_w < 0$, $M_q < 0$) across the speed range, and not just at 70 mph as noted previously. The derivative unique to the autogyro is M_Ω, and being negative, will *tend* to be stabilising. This is because an increase in rotorspeed will result in a nose-down moment, tending to reduce the axial flow through the rotor, and hence tending to reduce the original rotorspeed disturbance.

M_u is an indication of the speed stability of the aircraft, and the exhibited trend is consistent with the measured longitudinal stick position in trimmed flight. The propeller speed and hence thrust variations mentioned previously may very well have a role to play in this derivative, quite apart from the usual rotor and tailplane contributions. M_w is the angle of attack stability, and unusually for a rotorcraft, is negative throughout the speed range. This is an important derivative as it holds the

clue to a general understanding of autogyro flight dynamics. Unaugmented rotorcraft generally rely on a horizontal tailplane to provide $M_w < 0$. This is because the natural tendency of the rotor (and hence thrust vector) is to flap back with angle of attack, or w disturbances. Since rotor thrust also increases with w, and the thrust line usually passes close to the centre-of-mass in undisturbed flight, then both effects sum to produce $M_w > 0$, Ref. 24. However, the profile of M_u and M_q with speed would tend to suggest that the tailplane on this autogyro is somewhat ineffective, despite its relatively large size. This is consistent with wind tunnel tests on this configuration, Ref. 25.

Ref. 3 postulated that autogyro longitudinal stability could be dominated by the vertical position of the centre-of-mass relative to the propeller thrust line, and a configuration with propeller thrust line below the centre-of-mass could exhibit $M_w < 0$ even at low airspeeds where any tailplane contribution would be negligible. The mechanism for this is shown in Figure 8. The nose-up moment produced by a configuration with propeller thrust line below the centre-of-mass will require to be trimmed in equilibrium flight by having the main rotor thrust line passing behind the centre of mass as shown. In disturbed flight then, the possibility exists of the reduction in nose-down moment caused by the rotor flapping back, being overcome by the contribution from the increase in thrust, resulting in $M_w < 0$. Note that the result $M_\Omega < 0$ identified here is also consistent with such a configuration. Further validation of this postulate comes from the marked reduction in M_w (and M_Ω) at 50 mph. This is the about the minimum power speed, and roughly where the propeller thrust would be a minimum also. Any pitching moment from the propeller would therefore be a minimum, and the main rotor thrust line would be at its closest to the centre of mass in equilibrium flight, i.e. tending to give a smaller M_w than at the higher-power speeds of 30 and 70 mph.

Figure 9 shows three estimates for M_w at each speed, obtained from different flights. The multi-run consistency exhibited serves to confirm $M_w < 0$ throughout the speed range, even at low speed, and also the observed effect that M_w is reduced in magnitude at around the minimum power speed.

Figure 10 shows the identified derivatives in the rotor torque equation. It is impossible to relate these to any previous quantitative work. However, qualitatively T_u and T_w are consistent with Glauert's seminal work, Ref.4 in that an increase in airspeed and axial velocity will both tend to increase rotorspeed ($T_u > 0$, $T_w > 0$). Although the primary damping term T_Ω decreases with airspeed, the rotorspeed mode itself exhibits the opposite trend, Figure 6. This indicates the extent of inter-modal coupling between the rotorspeed and body degrees of freedom. Finally, the control derivative T_{η_s} shows that the rotorspeed response will become increasingly sensitive to control application with airspeed.

Discussion

The results are significant for several reasons. First, they are unique in that the literature indicates that no previous in-flight investigation of autogyro stability and control has taken place. Second, the results are timely in that the U.K. autogyro accident record is poor, and a substantial number of fatal accidents remain largely unexplained. In addition, the U.K.'s new airworthiness and design standard BCAR Section T is a unique code, and requires substantive data, having been developed largely from other codes. Third, contemporary flight test and data analysis techniques have been used, which helps to consolidate the status of system identification and parameter estimation for rotorcraft. The autogyro joins conventional single main and tail rotor helicopters, tandem rotor helicopters and tilt-rotors as rotorcraft that have enjoyed the successful application of these tools to a real engineering problem.

Although the results obtained are specific to the VPM M16 autogyro, they are of more general significance for two reasons. First, autogyro stability and control has not featured in the literature until recently, Ref. 3, and cataloguing the characteristics of one type benchmarks the quantification of autogyro stability in general. Second, the result in M_w in particular, can be rationalised in terms of centre of mass position with respect to propeller thrust line, an issue of direct relevance to all autogyros. The results can also be applied directly to the development of the airworthiness and design standard BCAR Section T, as they suggest some modification and amendment. First, the VPM M16 as identified fails to meet the short- and long-period dynamic stability requirements, despite this type enjoying a reputation for good handling characteristics. Second, there is no requirement for balance to be specified in terms of vertical centre-of-mass position in relation to the propeller thrust line. The results suggest that this is an important consideration in conferring positive angle of

attack stability M_w, which it is relatively easy to show has a key role to play in stabilising the phugoid mode of rotorcraft, Ref. 23.

Finally, the results quantify the extent to which the rotorspeed degree of freedom is significant in autogyro flight mechanics. The pilot relies on management of flight state to maintain rotorspeed, having no direct control over it. Although the results indicate that the rotorspeed mode is stable, it is closely coupled with the conventional rigid body degrees of freedom. The rotor torque derivatives indicate that rotorspeed is sensitive to airspeed and angle of attack perturbations and this may have implications for handling in marginal situations.

Conclusions

Robust identification of autogyro longitudinal stability and control derivatives has been possible using relatively straightforward frequency-domain parameter estimation tools.

Unusually for rotorcraft in general, the type examined displays classical longitudinal dynamic stability characteristics, and is stable throughout the speed range. However, rotorspeed is an important variable and is closely coupled with the conventional rigid-body degrees of freedom.

Interpretation of the identified stability derivatives indicates that the vertical position of the centre of mass in relation to the propeller thrust line may have an important role to play in autogyro longitudinal stability.

The results contribute directly to the development of the UK autogyro airworthiness and design standard, BCAR Section T in the important areas of dynamic stability, and weight and balance.

Acknowledgement

This work was conducted for the U.K. Civil Aviation Authority under Research Contract No. 7D/S/1125. The Technical Authority was Mr. David Howson.

References

1) Anon, "Airworthiness Review of Air Command Gyroplanes", Air Accidents Investigation Branch Report, Sept. 1991.

2). Anon, "British Civil Airworthiness Requirements, Section T, Light Gyroplane Design Requirements" Civil Aviation Authority Paper No. T 860 Issue 2, Jul. 1993.

3). Houston, S. S., "Longitudinal Stability of Gyroplanes", *The Aeronautical Journal*, Vol. 100, No.991, pp. 1-6, 1996.

4). Glauert, H., "A General Theory of the Autogyro", Aeronautical Research Committee Reports and Memoranda No. 1111, Nov. 1926.

5). Lock, C. N. H., "Further Development of Autogyro Theory Parts I and II", Aeronautical Research Committee Reports and Memoranda No. 1127, Mar. 1927.

6). Glauert, H., "Lift and Torque of an Autogyro on the Ground", Aeronautical Research Committee Reports and Memoranda No. 1131, Jul. 1927.

7). Lock, C. N. H., Townend, H. C. H., "Wind Tunnel Experiments on a Model Autogyro at small Angles of Incidence", Aeronautical Research Committee Reports and Memoranda No. 1154, Mar. 1927.

8). Glauert, H., Lock, C. N. H., "A Summary of the Experimental and Theoretical Investigations of the Characteristics of an Autogyro", Aeronautical Research Committee Reports and Memoranda No. 1162, Apr. 1928.

9). Wheatley, J. B., "Wing Pressure Distribution and Rotor-Blade Motion of an Autogyro as Determined in Flight", NACA TR 475, 1933.

10). Wheatley, J. B., "An Aerodynamic Analysis of the Autogyro Rotor with a Comparison Between Calculated and Experimental Results", NACA TR 487, 1934.

11). Wheatley, J. B., Hood, M. J., "Full-Scale Wind-Tunnel Tests of a PCA-2 Autogyro Rotor", NACA TR 515, 1935.

12). Wheatley, J. B., "An Analytical and Experimental Study of the Effect of Periodic Blade Twist on the Thrust, Torque and Flapping Motion of an Autogyro Rotor", NACA TR 591, 1937.

13). Schad, J. L., "Small Autogyro Performance", *Journal of the American Helicopter Society*, Vol.10, 1965.

14). McKillip, R. M., Chih, M. H., "Instrumented Blade Experiments Using a Light Autogyro", *Proceedings of the 16th. European Rotorcraft Forum,* Glasgow, Scotland, Sept. 1990.

15). Fu, K.-H., Marchand, M., "Helicopter System Identification in the Frequency Domain", *Proceedings of the 9th. European Rotorcraft Forum,* Sept. 1983.

16). Tischler, M. B., et al, "Demonstration of Frequency-Sweep Testing Technique using a Bell 214-ST Helicopter", NASA TM-89422, April 1987.

17). Tischler, M. B., "Frequency-Response Identification of XV-15 Tilt-Rotor Aircraft Dynamics", NASA TM-89428, May 1987.

18). de Leeuw, J. H., "Identification Techniques, Model Structure and Time Domain Methods", AGARD LS178, pp. 5-1 to 5-9, October 1991.

19). Kaletka, J., "Instrumentation and Data Processing", AGARD LS178, pp. 3-1 to 3-18, October 1991.

20). Tischler, M. B., "Identification Techniques, Frequency Domain Methods", AGARD LS178, pp. 6-1 to 6-4, October 1991.

21). Houston, S. S., Black, C. G., "On the Identifiability of Helicopter Models Incorporating Higher Order Dynamics", *AIAA Journal of Guidance, Control and Dynamics*, Vol. 14, No. 4, pp. 840-847, July-August 1991.

D. J., "Modelling Aspects and Robustness Issues in Rotorcraft System Identification", AGARD LS178, pp. 6-1 to 6-4, October 1991.

23). Padfield, G. D., "On the Use of Approximate Models in Helicopter Flight Mechanics", *Vertica*, Vol. 5, No. 3, 1981.

24). Bramwell, A. R. S., "Helicopter Dynamics", Arnold, London, 1976, pp. 199-200.

25). Coton, F.,et. al., "Wind Tunnel Testing of a 1/3rd. Scale Model Gyroplane", *Proceedings of the 20th. Congress of the International Council of Aeronautical Sciences,* Sorrento, Italy, Sept. 1996.

Figure 1 -- VPM M16 autogyro with instrumentation system fitted

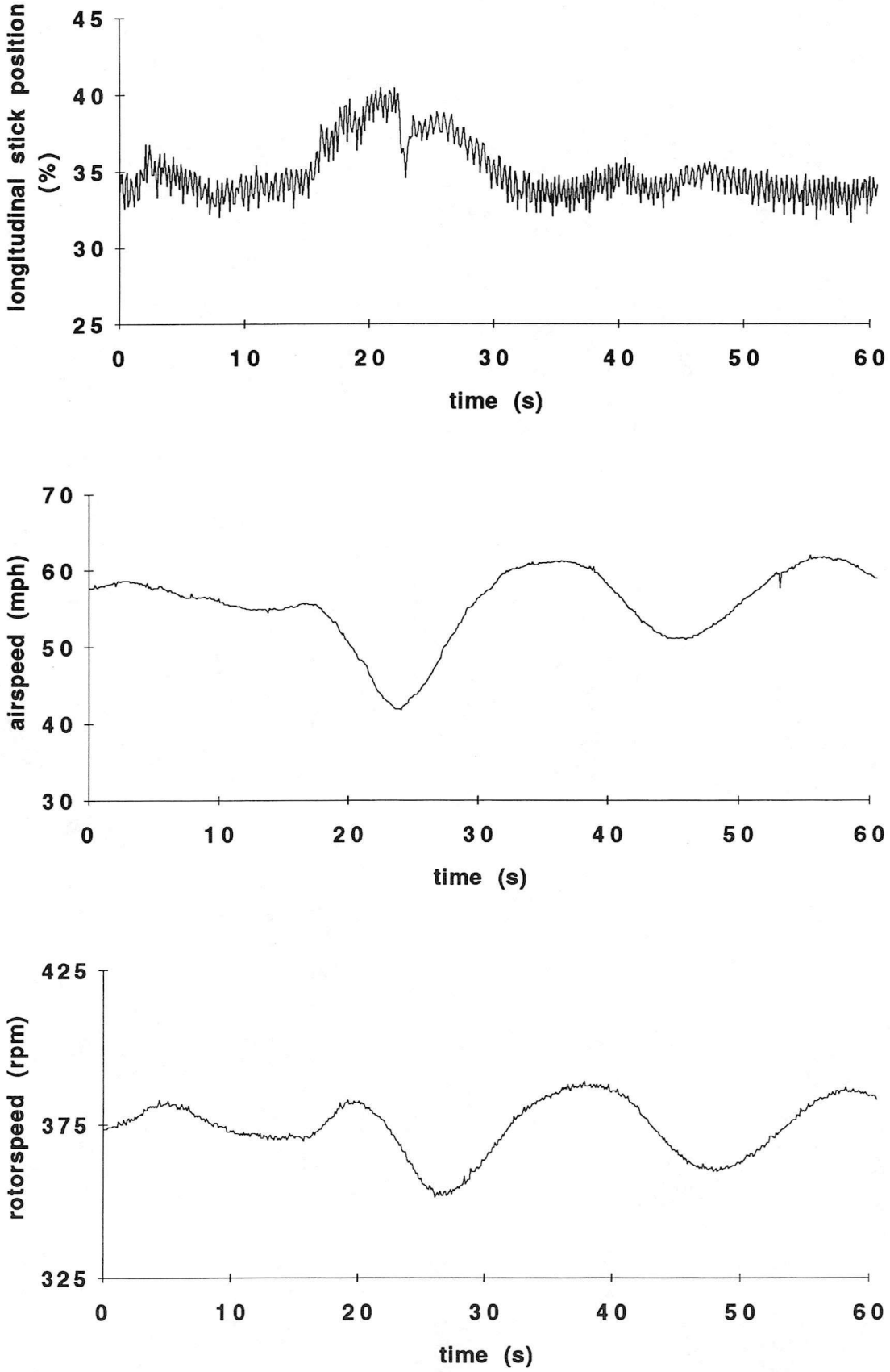

Figure 2 -- Response during phugoid test at 60 mph

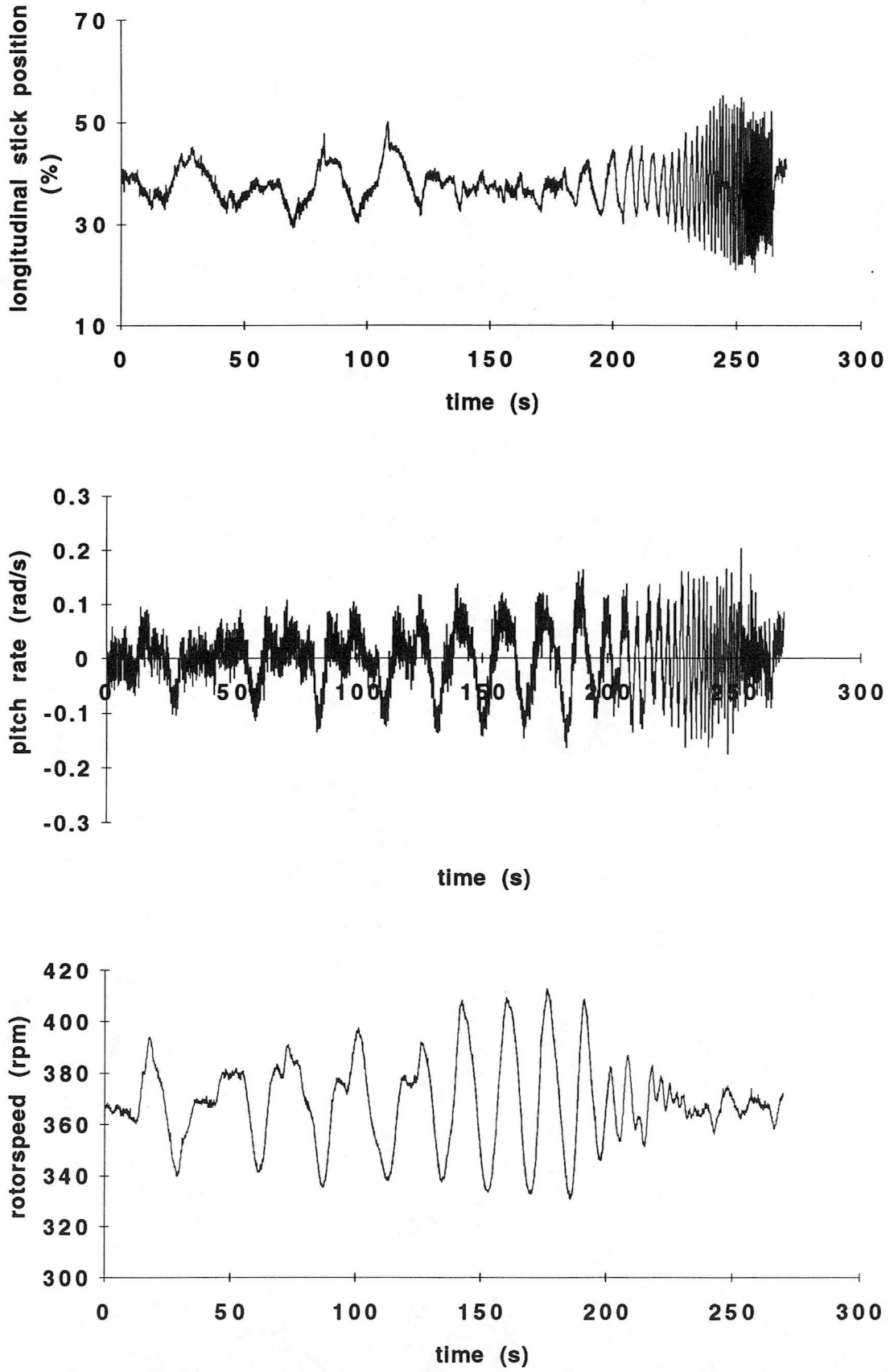

Figure 3 -- Response during frequency sweep test at 70 mph

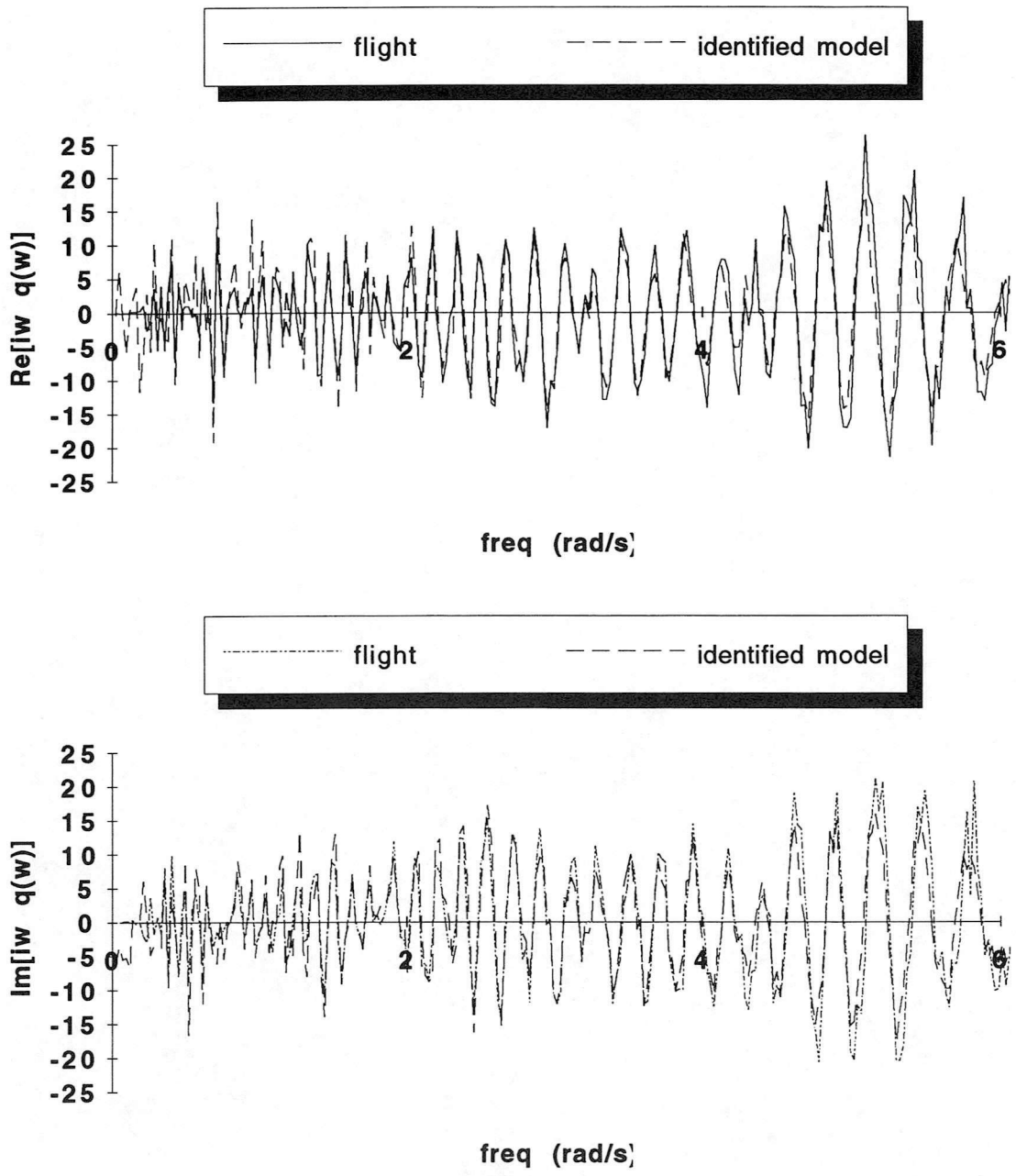

Figure 4 -- Fit quality of flight and identified model pitching moment equation

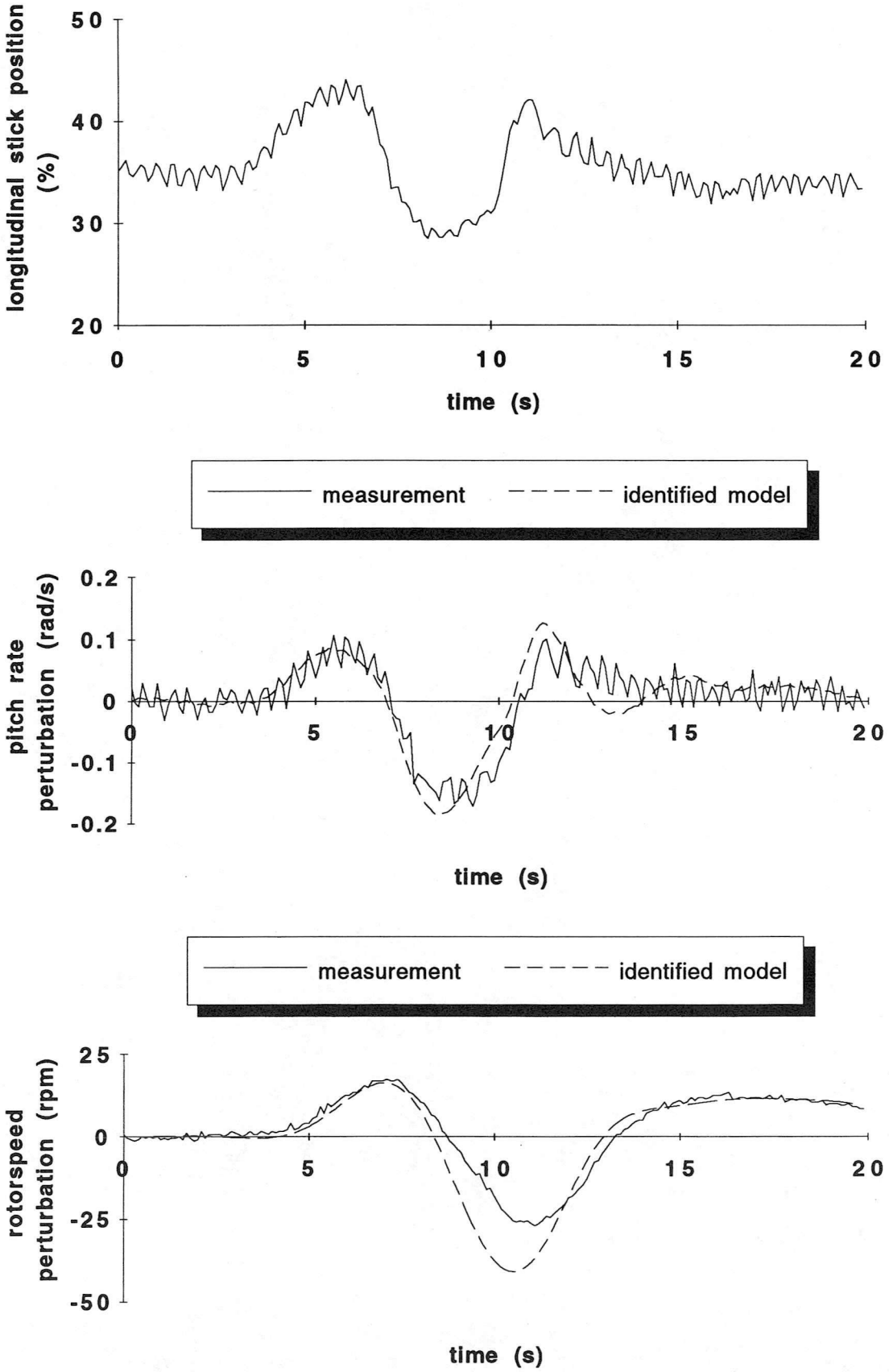

Figure 5a -- Identified model verification, 70 mph, short-period response

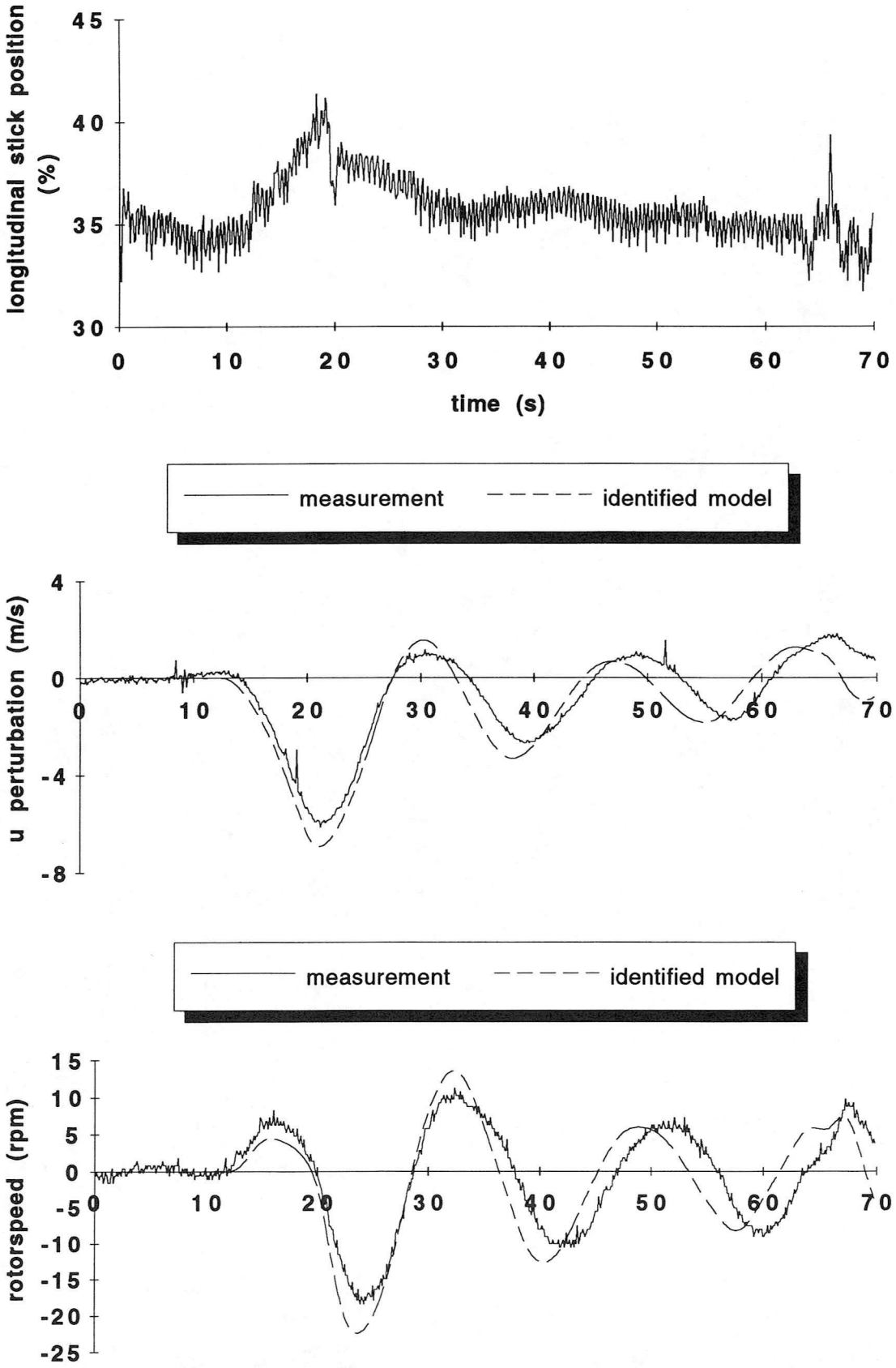

Figure 5b -- Identified model verification, 70 mph, phugoid response

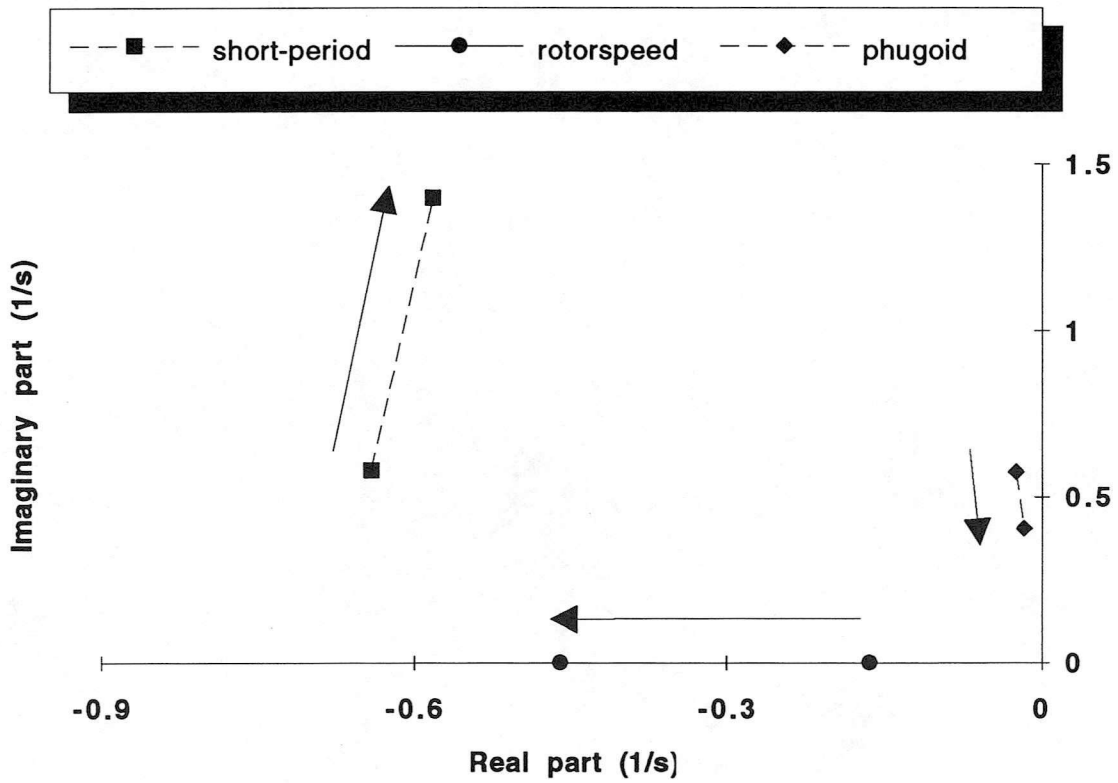

Figure 6 -- Identified model eigenvalues, 30, 70 mph

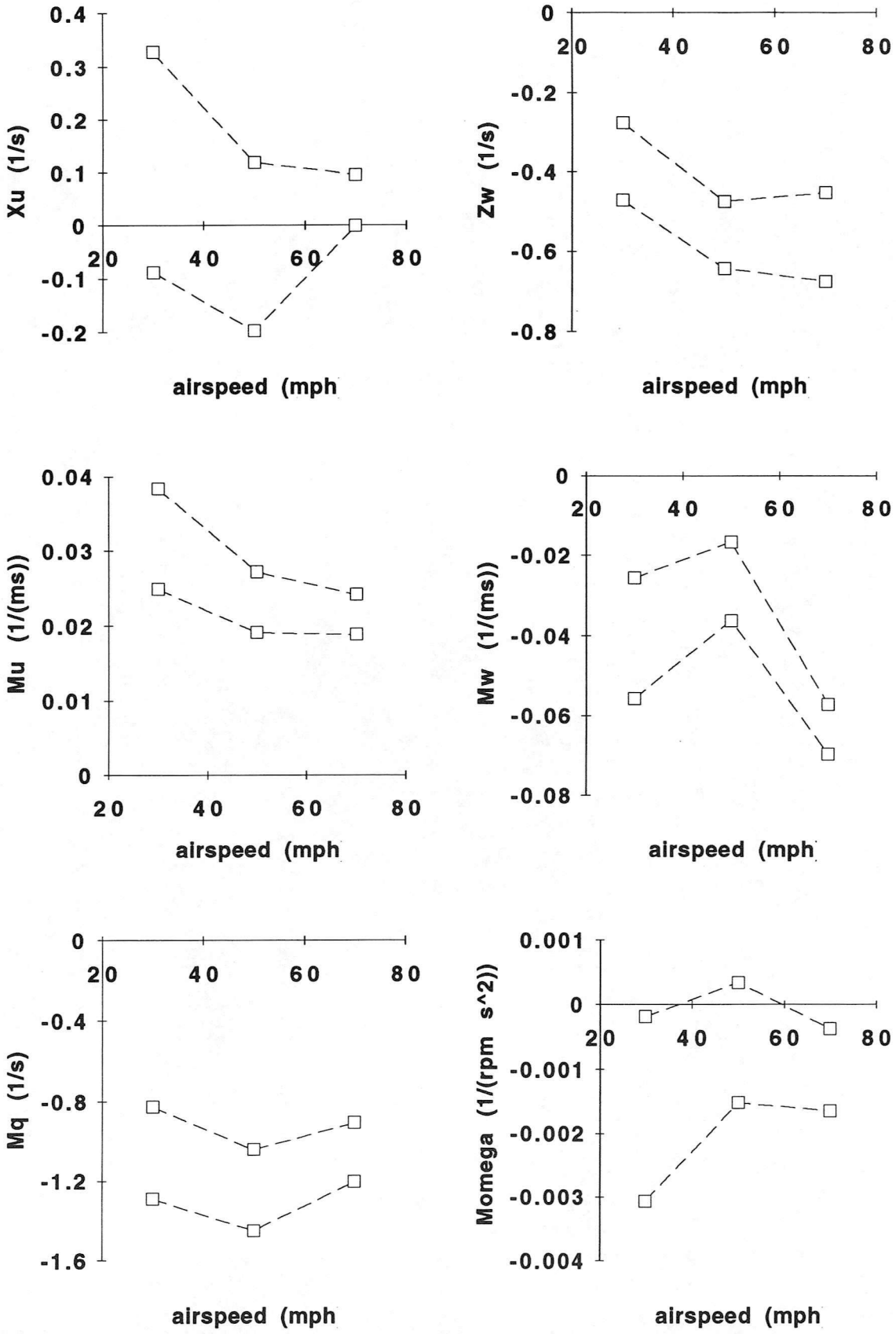

Figure 7 -- Key identified force and pitching moment derivatives

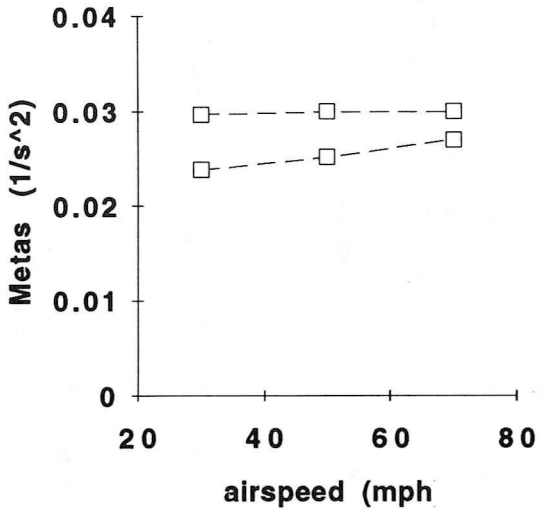

Figure 7 (concluded)-- Key identified force and pitching moment derivatives

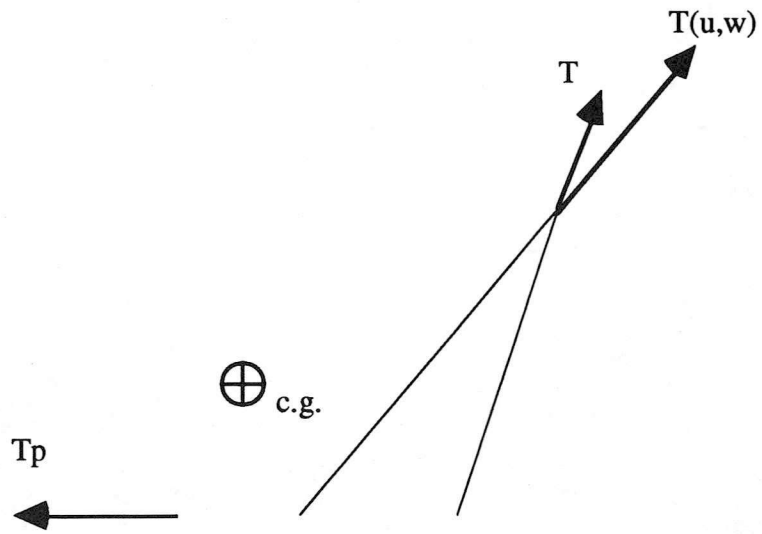

Figure 8 -- Rotor and propeller forces in equilibrium and disturbed flight

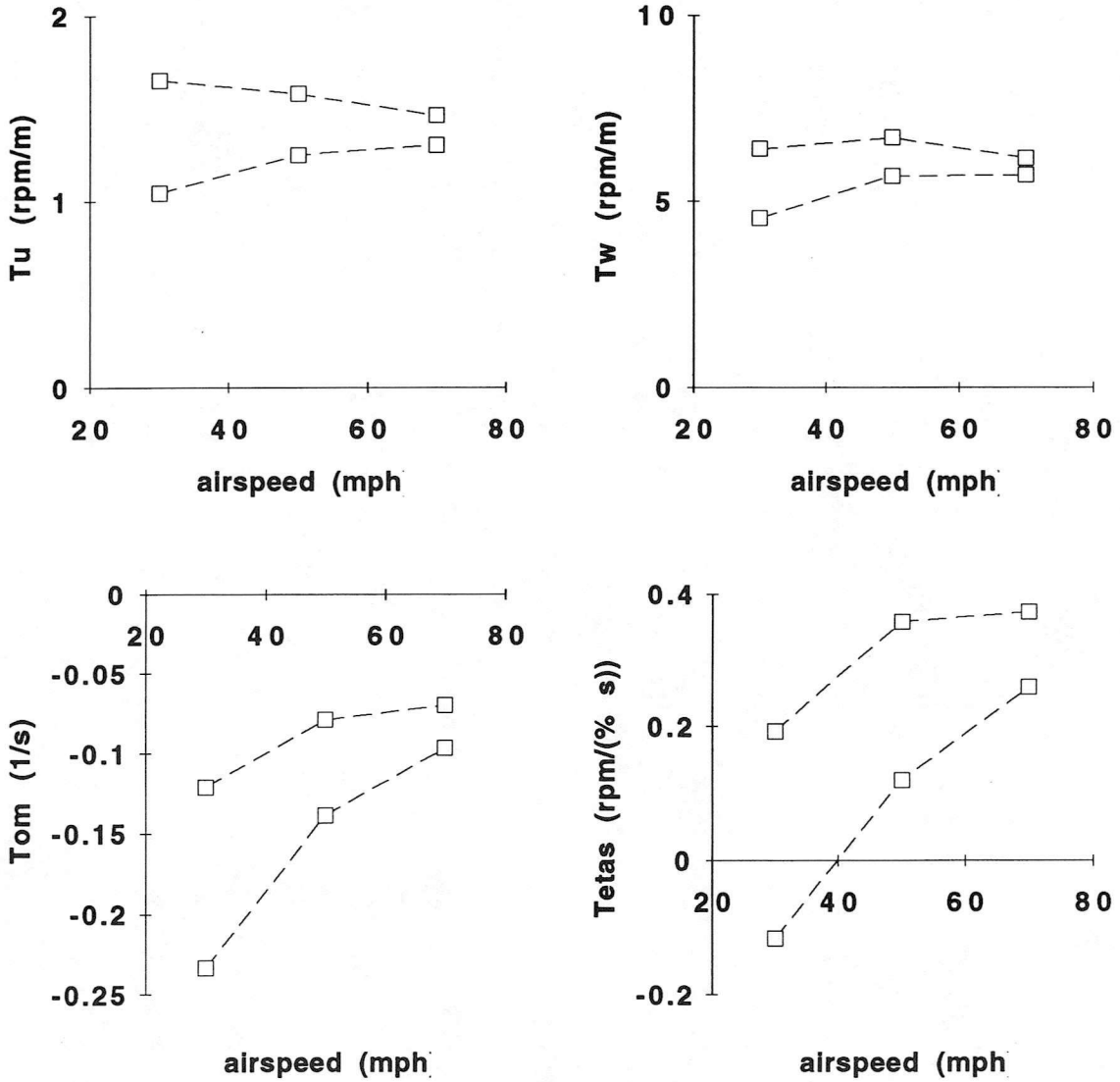

Figure 10 -- Rotor torque derivatives